

Robust superconducting correlation against inter-site interactions in the extended two-leg Hubbard ladder

Zongsheng Zhou,^{1,2,3} Weinan Ye,^{1,3} Hong-Gang Luo,^{1,3,4} Jize Zhao,^{1,3,*} and Jun Chang^{5,†}

¹*School of Physical Science and Technology & Key Laboratory for Magnetism and Magnetic Materials of the MoE, Lanzhou University, Lanzhou 730000, China.*

²*Beijing National Laboratory for Condensed Matter Physics and Institute of Physics, Chinese Academy of Sciences, Beijing 100190, China*

³*Lanzhou Center for Theoretical Physics and Key Laboratory of Theoretical Physics of Gansu Province, Lanzhou University, Lanzhou 730000, China.*

⁴*Beijing Computational Science Research Center, Beijing 100084, China*

⁵*College of Physics and Information Technology, Shanxi Normal University, Xi'an 710119, China*

The Hubbard and related models serve as a fundamental starting point in understanding the novel experimental phenomena in correlated electron materials, such as superconductivity, Mott insulator, magnetism and stripe phases. Recent numerical simulations indicate that the emergence of superconductivity is connected with the next nearest-neighbor hopping t' in the Hubbard model. However, the impacts of complex inter-site electron interaction in the t' -Hubbard model are less explored. Utilizing the state-of-art density-matrix renormalization group method, we investigate the t' -Hubbard model on a two-leg ladder with inter-site interactions extended to the fourth neighbor sites. The accurate numerical results show that the quasi-long-range superconducting correlation remains stable under the repulsive nearest-neighbor and the next nearest-neighbor interactions though these interactions are against the superconductivity. The ground state properties are also undisturbed by the longer-range repulsive interactions. In addition, inspired by recent experiments on one-dimensional cuprates chain $\text{Ba}_{2-x}\text{Sr}_x\text{CuO}_{3+\delta}$, which implies an effective attraction between the nearest neighbors may exist in the cuprates superconductors, we also show that the attractive interaction between the nearest neighbors significantly enhances the superconducting correlation when it is comparable to the strength of the nearest-neighbor hopping t . Stronger attraction drives the system into a Luther-Emery liquid phase. Nevertheless, with the attraction further increasing, the system enters an electron-hole phase separation and the superconducting correlation is destroyed. Finally, we investigate the effects of on-site Coulomb interaction on superconductivity.

I. INTRODUCTION

Despite the extensive investigations in the last decades, the microscopic mechanism of high- T_c superconductivity in cuprates remains one of the puzzles in condensed matter physics [1, 2]. Single band Hubbard model [3] and t - J model [4] are the simplest models frequently employed to understand experimental results in the high- T_c cuprates. The latter is the strong interaction limit of the former under hole doping, and is also the low energy effective model of the original three band d - p model [5], which directly depicts the physics on the CuO_2 plane in high- T_c cuprates. In the single band Hubbard model on a square lattice, many phases observed in high- T_c cuprates are reproduced, such as the antiferromagnetic magnetism at half filling [6–8] as well as the antiferromagnetic correlation upon hole doping [9], pseudogap [9–12], the stripe phase where charge density wave (CDW) and spin density wave (SDW) coexist around optimal doping [13, 14] and metal phase under overdoping [15]. It means that the Hubbard model captures some of the crucial ingredients of high- T_c cuprates.

Recently, it was found that the Hubbard model with an attractive nearest-neighbor (NN) interaction could well explain the results of angle-resolved photoemission spectroscopy on a one dimensional cuprates chain compound $\text{Ba}_{2-x}\text{Sr}_x\text{CuO}_{3+\delta}$ [16]. Due to various cuprates chain and

ladder materials, the Hubbard related models on chain and ladders have been extensively studied [17–27], which could help us understand the related experiments and gain insights into strongly correlated electron systems. However, for the simplest Hubbard model with a single orbital, the NN hopping along with on-site Coulomb interaction, current powerful numerical methods demonstrated that the ground state is not the superconducting state [14, 28], but a stripe phase with the wavelength of charge density $\lambda_c = 8$, which is recently observed in experiment [29]. Meanwhile, numerical results indicate the superconducting state is a high-energy excitation state and several stripe phases are highly competitive near the ground state [13, 28, 30–33]. These results imply that some crucial ingredients leading to the superconductivity are missing in the simplest Hubbard model. Some neglected terms, such as the hopping term beyond the NN sites and the inter-site interactions among electrons, should be taken into consideration to describe the physics of high- T_c cuprates. Indeed, the next-nearest neighbor (NNN) hopping term t' brings impressive change into the ground state, it does not only choose the wavelength of $\lambda_c = 4$ stripe state as the ground state [34] that is more widely observed in experiments [35–37], but also induce quasi-long ranged superconducting correlation on a four-leg cylinder [38–40]. Very recently, numerical simulations indicate that the t' -Hubbard model is adaptable in qualitatively capturing the physics in high- T_c cuprates [41].

In actual materials, it is worthy of noting that in one and two dimensions, the Coulomb screening is relatively weaker than that in three dimensions. Therefore, it is probably hard to thoroughly screen the long-range interactions among elec-

* zhaojz@lzu.edu.cn

† junchang@snnu.edu.cn

trons into on-site interaction, thus inter-site interactions are still considerable. And the hopping t' between the NNN sites can not be neglected directly either. Therefore, to have a better insight into the physics in cuprates, it is natural to consider the inter-site interactions in the t' -Hubbard model [42, 43]. The extended t' -Hubbard on ladders should be a more reasonable entrance in understanding the cuprates ladder materials exhibiting superconductivity [44–46]. Firstly, ladders serve as a bridge between one-dimensional and two-dimensional systems, in some cases, ladder share some similar physics with its two-dimensional counterpart. Secondly, due to the chemical similarities, a deep understanding on the cuprates ladder systems can also aid in comprehending the physics in two dimensional cuprates materials. Generally, we consider repulsive inter-site interactions in the extended Hubbard model as they originate from the Coulomb interaction. The situation may change when there exists a process for electrons exchanging virtual bosons, e.g. the electron-phonon coupling. For instance, the numerical simulation on the Holstein-Hubbard chain indicates that an effective attractive NN interaction can be mediated by long-range electron-phonon interaction [47]. Thus, it is also worthwhile exploring the t' -Hubbard model with attractive NN interaction.

Unearthing new contained physics and hunting for superconductivity in the Hubbard model are important research topics. Though the extended Hubbard model has been investigated [48–52], what the inter-site interaction will bring to the t' -Hubbard model is rarely explored at present. Here, focusing on a two-leg ladder and employing the density-matrix renormalization group (DMRG) [53–56] method, we investigate the effects of repulsive interaction on the superconductivity in t' -Hubbard model up to the fourth neighbor sites. Motivated by recent experiment [16], we also explore the influences of an effective NN attractive interaction on t' -Hubbard model. In the ladder systems, the numerical errors can be well controlled, so that high accurate numerical results are accessible. Our numerical results indicate that the superconducting correlation is slightly weakened but still robust under the repulsive NN and NNN interactions. The charge density distribution, density correlation, and spin correlations are nearly undisturbed as the long-range repulsive interactions are considered. In sharp contrast to the repulsive interactions, the attractive NN interaction significantly strengthens the superconducting correlation when the attraction is comparable with the NN hopping t . The spin and density correlations show a nonmonotonic dependence on the attractive interaction. Before the attractive interaction drives the system into electron-hole phase separation (PS), the coexistence of the algebraic superconducting and CDW correlations in the ground state is consistent with the Luther-Emery (LE) liquid [57]. In addition, analyzing the different components of pairing correlation, we find that the pairing symmetry tends to d -wave. At last, we study the impacts of on-site Coulomb interaction. Our numerical results show strong on-site interaction weakens the strength of superconducting correlation in the presence of both attractive and repulsive NN interactions. These results will be shown in detail in the later sections.

The content of the paper is organized as follows: Sec. II

involves a brief introduction of the model and some details of DMRG simulations. In Sec. III, we investigate the effects of repulsive and attractive NN interactions on the t' -Hubbard model. In Sec. IV, we probe the long-range repulsive interactions up to the fourth-neighbors. In Sec. V, with the present of NN repulsive and attractive interaction, we explore how the ground states affected by different on-site interaction U . This paper is closed by a summary in Sec. VI.

II. MODEL AND METHOD

The extended t' -Hubbard model on a two-leg ladder is written as

$$\mathcal{H} = - \sum_{\langle ij \rangle \sigma} t (c_{i\sigma}^\dagger c_{j\sigma} + h.c.) + \sum_{\langle\langle ij \rangle\rangle \sigma} t' (c_{i\sigma}^\dagger c_{j\sigma} + h.c.) + U \sum_i n_{i\uparrow} n_{i\downarrow} + \sum_{i \neq j} V_{ij} (n_{i\uparrow} + n_{i\downarrow}) (n_{j\uparrow} + n_{j\downarrow}), \quad (1)$$

where the first and second term in Eq. (1) represent electrons hopping between NN and NNN lattice sites, respectively, the coefficients t and t' are their hopping amplitude. $c_{i\sigma}^\dagger$ ($c_{i\sigma}$) creates (annihilates) an electron at site i with spin σ . The third term is on-site Coulomb repulsion for two electrons with different spins, in which $n_{i\sigma}$ is the number of electrons with spin σ . The last term describes the interaction among electrons at different sites. Generally, V are positive due to the repulsive long-range Coulomb interaction between electrons. However, the recent experiment implies that the effective interaction between NN sites could be attractive [16]. Therefore, to investigate how the inter-site interactions affect the ground state properties, we consider both repulsive and attractive inter-site interactions. For repulsive interaction, the inter-site interactions are considered up to the fourth neighbor, and in the attractive case, we only consider NN interaction. We assume the values of V_{ij} only depend on the distance between site i and j . To be visually intuitive, we illustrate the model Eq. (1) in Fig. 1.

In this work, we simulate the model Eq. (1) by utilizing the DMRG method, which has been shown as the most powerful method to study one or quasi-one dimensional systems. In numerical calculations, we set the NN hopping amplitude $t = 1$ as the energy unit, the second neighbor hopping amplitude $t' = -0.25$, and the on-site Coulomb interaction $U = 8$

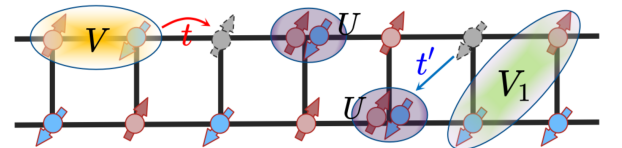


FIG. 1. A sketch diagram of the extended t' -Hubbard model on a two-leg ladder. t and t' represent the nearest and the next nearest neighbor hopping amplitudes, respectively. U is on-site Coulomb repulsion. V and V_1 are the NN and the NNN inter-site interactions. Inter-site interactions beyond NNN are not shown here.

unless explicitly noted. These values are frequently used in related numerical simulations for high- T_c cuprates. The numbers of electrons with spin-up and spin-down in (1) are conserved respectively, in the calculations, the two $U(1)$ symmetries are implemented to lower the numerical costs. We retain up to 8000 states and the largest truncation error on the order of 10^{-7} , at least 20 sweeps are implemented to make sure the calculations are well converged. The convergence of our DMRG results also checked by the ground state energy, expectation values of observations, and the von Neumann entropy. Our DMRG code is based on the ITensor library [58].

We adopt open boundary conditions in all the calculations. The system has $N = 2 \times L$ sites and the largest system size we simulated reaches $L = 96$. At half filling, strong on-site interaction freezes the charge degree of freedom and the ground state is Mott insulator. Hole doping makes the magnetic order in the insulator unstable and drives the system into unconventional phases, probably including superconductivity. The filling factor is defined as N_e/N , where N_e is the electron number. The concentration of hole is $\delta = 1 - N_e/N$. Here, we focus on the case where the hole concentration around $\delta = 12.5\%$.

III. NN INTERACTION

Though some crucial characters of high- T_c cuprates are captured by the simplest Hubbard model and t - J model, more and more numerical evidences indicate the models are oversimplified and insufficient to explain some experimental results of cuprates. Some neglected subleading terms, such as electron hopping beyond the nearest neighbor as well as inter-site interactions, may be responsible for some puzzling novel phenomena. For example, the NNN hopping t' induces quasi long-range superconductivity in the ground state [38]. In actual strongly correlated materials, the inter-site interactions are hard to be totally screened, and these interactions may also affect the properties of the system. As the NN interaction is the most remarkable one except the on-site interaction, in this section, we investigate the effects of NN interaction on the t' -Hubbard model. The interactions are intuitively repulsive as they result from Coulomb force between electrons. However, recent experiment on a one-dimensional cuprates chain implies electrons in NN sites may feel an effective attraction. So, we consider both repulsive and attractive NN interactions.

A. numerical convergency

Before discussing the results of NN inter-site interactions, we briefly display the convergence of DMRG calculations and some details in fitting the DMRG results. For simplicity, we take the results of NN interaction $V = 0.4$ as a representative sample as shown in Fig. 2, the convergence of the calculations under other parameters are similar. To diagnosis the possibility of superconductivity, the singlet pairing correlation is defined as

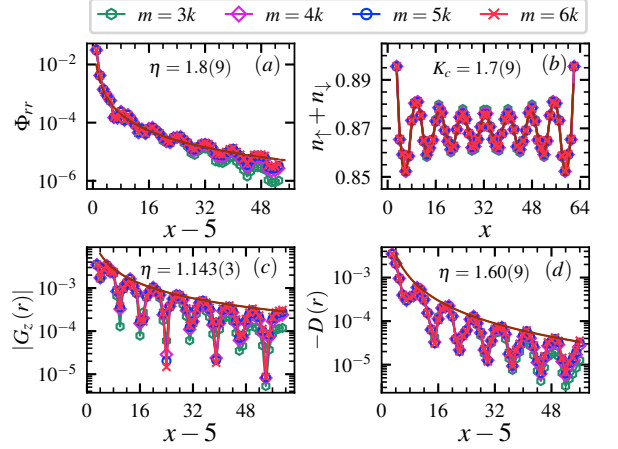


FIG. 2. Convergence of DMRG results for $V = 0.4$ as a representation. Panel (a) shows the pair-pair correlation between rungs. The brown line in (a) is a fitting via a power decay function, the solid part represents the data used to obtain the power function, and the dashed parts are extrapolated data from the power fitting. Panel (b) displays the charge density profile, the brown wavy line is the fitting via the function $n(x) = n_0 + A \cos(Qx + \phi)$, where $A = A_0 [x^{-K_c/2} + (L_x + 1 - x)^{-K_c/2}]$ and Q are the amplitude and wave vector of CDW, respectively. (c) and (d) is the spin-spin and density-density correlation, respectively, the brown line in the two subfigures are power fittings of points on the top of swellings. All these results indicate that 4000 retained state is large enough to make our DMRG simulations well converged. The common legend are shared by these subfigures.

$$\Phi(x) = \langle \Delta^\dagger(x_0) \Delta(x_0 + x) \rangle. \quad (2)$$

Here, the variable of the pairing field denotes the position of a bond on leg or rung. For example, when we consider the pairing correlation between rungs, the spin singlet pair-field creation operator $\Delta^\dagger(x)$ is given by $\Delta^\dagger(x) = \frac{1}{\sqrt{2}} [c_{(x,0),\uparrow}^\dagger c_{(x,1),\downarrow}^\dagger - c_{(x,0),\downarrow}^\dagger c_{(x,1),\uparrow}^\dagger]$, where the site index is labeled by the rung index x and leg index $y = 0, 1$, respectively. Similarly, the charge density profile is $n(x) = 1/2 (n_{x,0} + n_{x,1})$, S_z component of spin correlation $G_z(x) = \langle S_{x,i}^z S_{x_0,i}^z \rangle$, and charge density correlation $D(r) = \langle n_{x,i} n_{x_0,i} \rangle - \langle n_{x,i} \rangle \langle n_{x_0,i} \rangle$. The number of retained states m ranges from 3000 to 6000 with an increment of 1000. When the number is greater than or equal to 4000, all the results have a good convergence such that their differences are tiny as shown in Fig. (2). Therefore, 4000 retained states are sufficient to obtain accurate numerical results, and there is no need to extrapolate the DMRG results to the $m = \infty$ limit. In the later DMRG calculations, we keep at least 4000 states to ensure the numerical accuracy. The brown lines in Fig. (2) are the fittings of corresponding data. Power decay functions can fit the correlation functions well, and the charge density profile can be fitted via a trigonometric function multiplied by a spacing-dependent amplitude given in Fig. 2. The spin and

charge correlations behave in a spatial oscillation with considerable amplitudes, so we use the points on the top of each upward bulge to obtain the power function. In the following discussion, we will not involve the details of fittings any more and directly use the power exponent extracted from the power function.

B. repulsive interaction

Next, we add the NN repulsive interaction. Fig. 3 shows the effects of repulsive V term on the charge density profile, density correlation, spin correlation, and the superconducting correlation between rungs. The strength of V exhibited here ranges from 0.2 to 0.8 with a step of 0.2, the left column and right column in Fig. 3 correspond to the results of two different system sizes $L = 64$ and $L = 96$, respectively. The quantities shown here share the same behaviours for the two sizes, so the finite size effects are minor and should not qualitatively alter our conclusions. Firstly, as shown in Fig. 3 (a), (c), and (e), the charge density profile, density correlation, and spin correlation are insensitive to V . Under various V , each of the behaviours can be approximately fitted by a single function. The CDW is robust in the presence of NN Coulomb interaction, only the charge densities close to the boundaries are slightly affected as we adopt the open boundary conditions. Clearly, from Fig. 3 (a) and (b) the wavelength of charge density is $\lambda_c = 8$, and there is one hole in each stripe. Analyzing the spin correlation function, we find that there are domain walls in the antiferromagnetic background where holes are enriched. The period of spin order λ_s is about 16, twice of the charge density wave. Secondly, the last row subfigures (g) and (h) in Fig 3 indicate that the superconducting correlation is susceptible to the repulsive NN interaction. For the both system sizes, a larger power exponent of the function is required to fit the superconductivity correlation function when the strength of repulsive NN interaction is increased. Thus, the superconductivity is weakened by repulsive NN Coulomb interaction. At last, the numerical results show that the superconductivity is stable against the repulsive NN interaction, though the NN interaction weakens the superconducting correlation, as shown in Fig. 3, instead of damaging the superconductivity. For larger V , even if $V = 1.6$ (not shown), the superconductivity correlation still obeys a power decay function.

For the t' -Hubbard model with only on-site interaction, the Luttinger parameter K_c of CDW, extracted from the CDW function given in Fig. 2, is comparable to the Luttinger parameter of superconductivity or the decay exponent of superconducting correlation. The superconducting correlation is weakened by NN repulsive interaction. Though superconductivity and CDW coexist in the ground state, with the increase of repulsive NN interaction, the CDW dominates in the ground state.

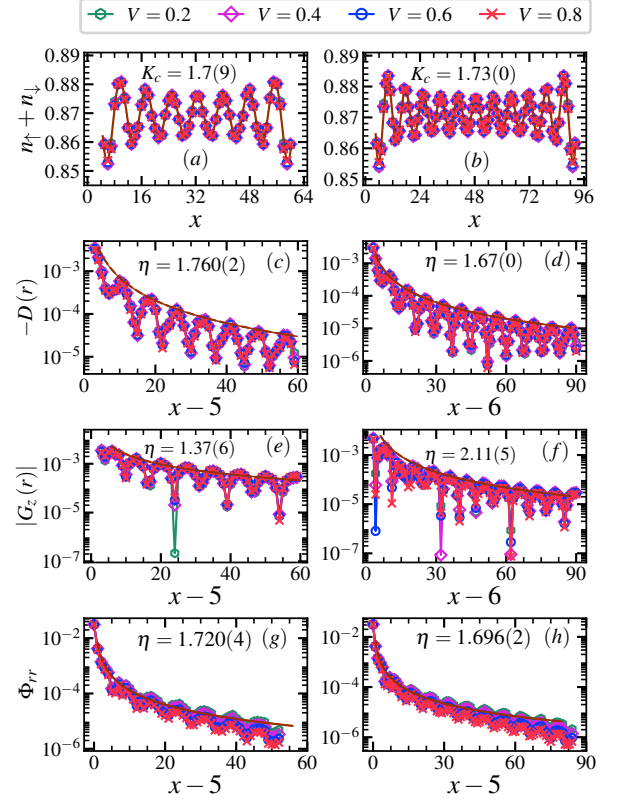


FIG. 3. The charge density profile, density correlation, spin correlation, and superconducting correlation under different strengths of repulsive NN interaction, V ranges from 0.2 to 0.8 with an increment of 0.2. The left column is the results of $L = 64$, the results of $L = 96$ are shown in the right column, the DMRG results on these two system sizes are well consistent. The brown lines in these figures are power fittings of the results of $V = 0.2$. In (a) and (b), the points close to boundaries are dropped, but all the valleys and peaks are retained, from which we can easily obtain the wavelength of CDW. The y -axes in the subfigures in each row share the same labels. All these subfigures shares the same legend.

C. attractive interaction

The numerical results in above indicate that the ground state is not inclined to superconductivity at the presence of repulsive inter-site interactions. Recently, some experimental spectra characteristics of a one-dimensional cuprates chain can be well understood via the Hubbard model with attractive NN interaction. Furthermore, numerical simulation have identified that an effective attractive interaction is induced in the Holstein-Hubbard model with long-range electron-phonon coupling. The experimental and numerical work renewed people's interest in Hubbard model with attractive NN interaction [59–63]. In the one-dimensional chain, the ground state exhibits p -wave superconductivity [60]. And the correlation of d -wave superconductivity is enhanced by attractive interaction on a four-leg cylinder [61]. Here, we consider the Hubbard model with attractive NN interaction on the two-leg ladder.

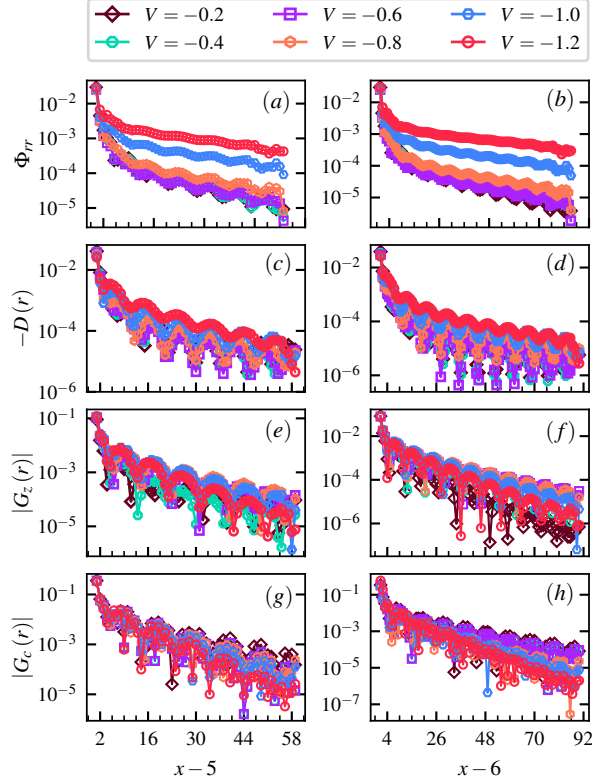


FIG. 4. The left column and the right column are the results of system sizes $L_x = 64$ and $L_x = 96$ under different attractive NN interaction, respectively. The numerical results of the two system sizes are well consistent. (a) and (b) are the superconductivity correlation, it is enhanced with the increase of V . The enhancement of superconductivity becomes remarkable when the strength of V is larger than 0.6. The density correlation function, shown in panels (c) and (d), always decays algebraically. In panels (e) and (f), the spin correlation changes from a algebraic decay into an exponential decay with the increase of V , indicating the open of spin gap. (g) and (h) show the single particle Green function, it decays algebraically under small V , but exhibits an exponential decay as V becomes strong, which implies the open of charge gap when strong attractive V is introduced. The subfigures (a)-(h) use the same legend.

der. Through extensive numerical simulations, we give more insights on how the spin correlation, density correlation, and the superconducting correlation are affected by the attractive interaction. Cooperating with recent numerical simulations, we can gain a deeper understanding of the Hubbard model with attractive interaction.

Following the case of NN repulsive interaction, we also take two system sizes $L = 64$ and $L = 96$ to show the numerical results. The main results are summarized in Fig. 4. The numerical results on the two systems sizes are well consistent. The superconducting correlations for the two systems are shown in Fig. 4 (a) and (b). When the strength of $V < 0.6$, the attractive interaction has no obvious effects on the superconducting correlation. With increasing of V , the superconducting correlation shows a slower and slower decay, indicating a significant enhancement by strong attractive V . The spin

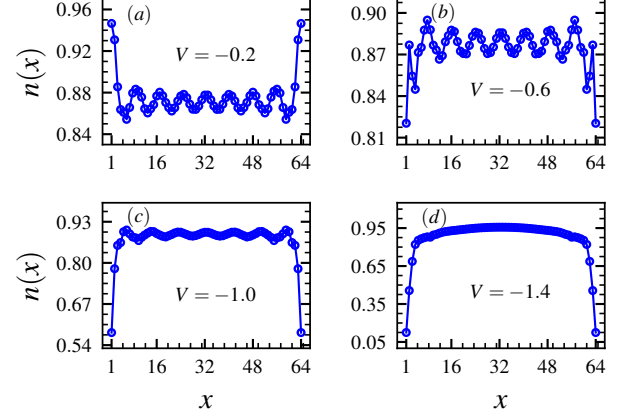


FIG. 5. Typical charge density distributions under different V with the system size $L_x = 64$. Since open boundary condition are implemented, electrons prefer to accumulate at the boundaries for small V , while holes on the boundaries are favorable when V is large. If V is not strong enough, as show in (a), (b), and (c), the modulation of charge density is maintained. In the panel (d), The modulation is destroyed by strong NN attractive interaction, electrons are gather in the bulk and the holes are at the two edges, indicating a phase separation.

correlation is enhanced by weak V while weakened by strong V . Meanwhile, the decay of the weakened spin correlation changes from a power law to an exponential law, which indicates the spin order is quenched by the strong attractive interaction. The charge density correlation is slightly weakened by small V but it is strengthened by strong V , which is a contrary to spin correlation. The different dependencies of spin correlation and superconducting correlation on V indicates that a competition exists between them. For large V , the valleys in density correlation become shallow, as shown in Fig. 4, and the charge density distribution cannot be fitted by the function for CDW used in Fig. 2 at large V . The exponential decay of spin correlation and single particle Green's function show that both the spin and charge excitations are gapped. In addition, the density correlation obeys a power decay behaviour. These indicate large V drive the system into an LE liquid phase. After the V drive the system into the LE liquid, the superconductivity is significantly enhanced. For very strong NN attractive interaction, the system is driven into electron-hole SP, which is characterized by regions with rich holes and regions with rich electrons. Due to the attractive NN interaction and OBC in our DMRG simulation, the holes prefer to accumulate in the two edges for strong attraction, while the electrons tend to gather in the inside. The evolution of charge density distribution under different attractive V is shown in Fig. 5.

D. pairing symmetry

At the end of this section, we briefly discuss the pairing symmetry on the two-leg ladder. Though the two-leg ladder does not have the same spatial symmetry in the two direc-

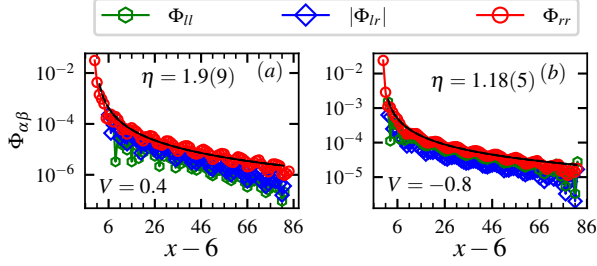


FIG. 6. Three different superconducting correlations, the singlet pairing correlation between a reference rung bond and bond on rungs Φ_{rr} , and bonds on one leg Φ_{rl} , as well as two bonds on the same leg Φ_{ll} , for $V = 0.4$ and $V = -0.8$ with $L = 96$ are shown. Since the constraint of ladder geometry, we only show the long range part of Φ_{rl} and Φ_{ll} . The long-range behaviors of the correlations in the two cases tell us d -wave superconductivity are favored in the ground state. These two subfigures share the same legend.

tions along leg and rung, through pairing correlations we may still gain some sights about the pairing in the two-dimensional case. Here, three different superconductivity correlations, $\Phi_{rr}(x - x_0)$, $\Phi_{rl}(x - x_0)$ and $\Phi_{ll}(x - x_0)$, are used to diagnosis the pairing symmetry, where the index r and l represent the bond in the rung and leg respectively. The first index represents the reference bond at position x_0 , and the second index represents the other bond at x . The superconductivity correlation for two typical V are shown in Fig. 6, they satisfy the characters of d -wave symmetry. These results mean that for the t' -Hubbard model, with the presence of repulsive or attractive NN interaction, the superconductivity tends to be d -wave. When the strength of NN attractive interaction is comparable to NN hopping t , the d -wave superconductivity is significantly enhanced. The dependency of superconductivity on the strength of NN attractive is consistent with recent DMRG simulation on a four-leg square cylinder [61], which confirm that a d -wave superconductivity may be stabilized by NN interaction in two-dimensional square lattice.

IV. LONG-RANGE INTER-SITE INTERACTION

Now we consider the inter-site Coulomb interaction beyond the NN sites, ranging to the fourth neighbor sites. In following calculations, we set NN interaction $V = 0.8$. The results of $L_x = 64$ are shown in Fig. 7. The superconducting correlation is shown in panel (a) of Fig. 4. With the increase of the NNN interaction from $V_1 = 0.4$ to $V_1 = 0.6$ the superconducting correlation is suppressed slightly. With $V_1 = 0.6$ and the long-range third and fourth neighbor interactions involved, the superconducting correlation nearly remains unaffected as shown in the legend of Fig. 7 in the form of (V_1, V_2, V_3) for the specific values of the interactions strength. Just like the case of NN interaction, the power decay function gives a better fitting of the superconducting correlation than the exponential function, indicating the robustness of the superconductivity correlation to the complex interactions. In the whole

process, the charge density profile (not shown), density correlation, spin correlation, as well as the single-particle Green function are insensitive to these repulsive interactions. If we take a closer look, the strengths of density correlation and single particle's Green function are subtly suppressed by these long range interactions, while these long range inter-site interactions marginally enhance the strength of spin correlation. Except the single-particle Green function, which decays exponentially, both spin and density correlations decay algebraically.

Based on these simulations, we can conclude that the ground state properties of t' -Hubbard model are quite robust to these long-range repulsive inter-site interactions. Though the inter-site repulsion between electrons tends to weaken the superconductivity, the algebraic superconducting correlation is not destroyed by the inter-site interactions, even if the strengths of these interaction are comparable or much stronger than the strength of t . Since these repulsive inter-site interactions always tend to weaken the superconductivity, reducing these repulsive interactions should be beneficial for the superconductivity.

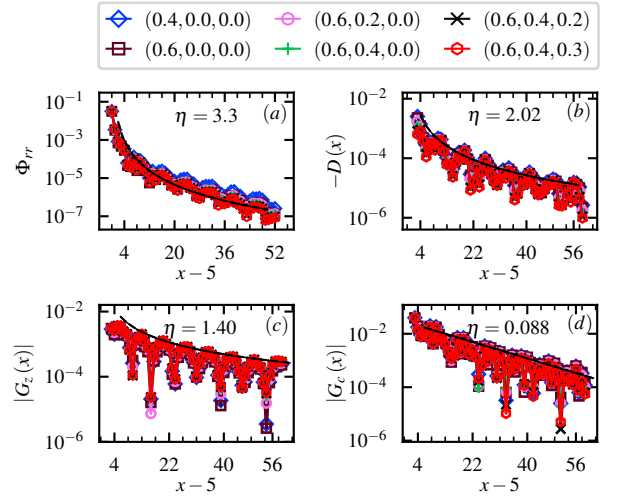


FIG. 7. Correlation functions when repulsive inter-site interactions beyond the NN neighbor are taken into account. The legend represent the values of inter-site interaction in the form of (V_1, V_2, V_3) , which are shared by these subfigures. Panel (a) is the superconducting correlation between rungs, the repulsive NNN interaction V_1 will slightly weaken the correlation. For the third neighbor and the fourth neighbor interactions, the superconductivity correlations are nearly the same. Meanwhile, the superconductivity correlation is hard to be fitted by an exponential decay function, the power decay functions gives a better fitting. The spin correlation function, density-density correlation, and single particle Green function, shown in (b), (c), and (d) respectively, are insensitive to these interactions, both the spin correlation and density correlation obey power law decay. But the single particle Green function decays exponentially.

V. VARIATION IN ON-SITE COULOMB INTERACTION

At last, we investigate the effects of on-site Coulomb interaction. On the one hand, when electrons in materials are less localized, the band width can be larger so that a smaller relative U should be considered. On the other hand, people are also interested in the physics of large U limit of Hubbard model under doping. For simplicity, considering both repulsive and attractive NN interaction with $|V| = 0.4$, we vary the strength of on-site Coulomb interaction from 2 to 14 with an increment of 2, all the other parameters in the extended Hubbard model are fixed. For clarity, we mainly show the results of $U = 4, 8, 12$ in Fig. 8.

Despite some minor differences in the two cases, the charge density profile, and the correlations shown in Fig. 8 share many common behaviors on the dependency of the Hubbard U , which are expected to the properties of t' -Hubbard model itself. Firstly, the superconducting correlation is enhanced as U is reduced and tends to be saturated. For example, the strength of superconducting correlation of $U = 4$ is almost the same as the one of $U = 2$. Secondly, the wavy charge density distribution is supported when U is around 8, while under both stronger and smaller U , it becomes unstable, the amplitude of inhomogeneous distribution reduced and the wavy feature disappeared. The instability under very large U agrees with a previous result of Hubbard model on a four-leg cylinder [40]. The CDW collapses when $U = 12$ for repulsive V , but it still exists for attractive V and cracks until we further increase U . These indicate the CDW under attractive V is more stable against the interference of large U . The CDW also destabilizes when a smaller U is considered. Though the charge density undulates, it starts getting close to a uniform distribution. Our results imply that uniform superconductivity is likely to form under small U . Here, the numerical results give the tendency that the superconductivity and stripe is not tightly related in the t' -Hubbard model on a two-leg ladder. The superconducting correlation is established at small U , though increasing U weakens its strength, the power decay behavior is robust in the whole range of U we considered here. CDW is induced until U reaches certain strength and it is damaged at large U .

Under the two situations, the density-density correlations, spin correlations as well as the single particle Green's functions obey a power law decay behavior, implying the spin excitation and charge excitation are gapless. The density correlation is slightly suppressed with the increase of U . Compared with attractive V , the density-density correlation are easier weakened under repulsive V . The spin correlation is enhanced at first and then is suppressed when U increases, and it has a wilder window of enhancement for repulsive V . The single particle Green's function is overall weakened as we increase U , it is more sensitive under repulsive V .

VI. CONCLUSIONS

Using the DMRG method, we have systematically investigated how the complex interactions affect the ground state of

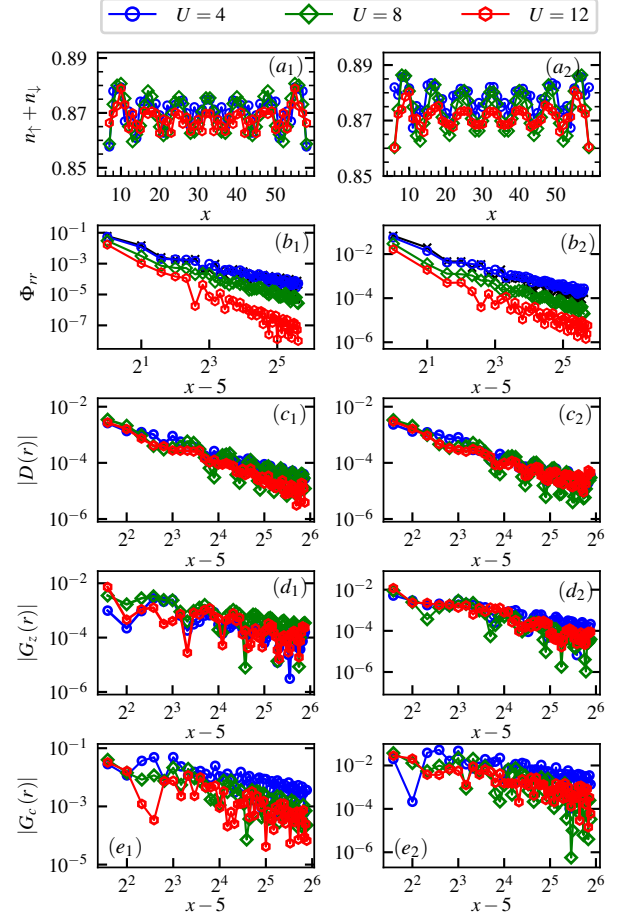


FIG. 8. When the system size $L = 64$, the left column and the right column are the results under different Hubbard U when the NN interaction $V = 0.4$ and $V = -0.4$, respectively. Subfigures (a_1) and (a_2) are the charge density distributions, the CDW order is stabilized under medium-strength of U , where $U = 6, 8, 10$. (b_1) and (b_2) show the superconducting correlation, large U tend to weaken the strength of the correlation. Under same U , the strength superconductivity correlation of repulsive V is weaker than the one of attractive V , the data in black is the results of $U = 2$. The density correlations are given in (c_1) and (c_2) , they decay algebraically and slightly weakened overall with the increment of U , and it is easier weakened under repulsive V . The spin correlations are shown in panels (d_1) and (d_2) , they are enhanced at first and suppressed when U is large, the spin correlations in the two cases satisfies a power decay. In the last row, (e_1) and (e_2) , the single particle Green's functions are suppressed with the increase of U , it is easier to be weakened when increasing U for repulsive V than for attractive V , the legend are shared by all the subfigs, for clarity, the data of $U = 2, 6, 10$ are not shown.

the t' -Hubbard model on a two-leg ladder. Without inter-site interactions, the superconducting order and the CDW order are comparable. The NN repulsive interaction weakens the superconductivity order and leads to the domination of CDW. When the long range Coulomb interaction is well screened it is more likely to induce superconductivity. Our numerical results show that the ground state properties are stable against on

the longer-range repulsive interactions. The exact numerical results clearly indicate repulsive interactions between different sites are adverse to the superconductivity. However, the superconductivity in t' -Hubbard is not damaged by physical reasonable repulsive inter-site interactions on a two-leg ladder.

Motivated by recent experimental results as well as the numerical simulations, we also investigated the attractive NN interaction on a two-leg ladder. The numerical results show that both the spin order and charge order are sensitive to the attractive interaction, though the superconductivity is less affected when V is small. But for relatively large V the superconductivity order is significantly enhanced. For very large V , the system evolves into phase separation. Before entering the phase separation, we find an LE liquid phase. Our numerical results show strong evidence that the superconductivity is strengthened by strong attractive NN interaction, and it is considerably enhanced when the strength of V is comparable to the NN hopping amplitude t , agreeing with a recent DMRG study on a four-leg cylinder.

When the superconductivity is quasi-long ranged, by analyzing the different singlet pairing correlations, we find the superconductivity tends to be d -wave. Both in repulsive and attractive interactions, the superconductivity is unfavorable under strong Hubbard interaction U . In addition, the charge density wave is supported when U is around 8, both weaker and stronger U make the charge density unstable.

We have extensively explore the effects of complex inter-site interaction on the superconductivity of t' -Hubbard model on a two-leg ladder. As there exist superconducting cuprates ladder materials, our numerical results can be helpful in understanding the novel physics in these materials. Ladder serves as a bridge between one and two dimensional systems, our results can also shield some lights on revealing the high- T_c superconductivity in cuprates.

Acknowledgments: This work is supported by the National Key Research and Development Program of China (Grant No. 2022YFA1402704) and by the National Natural Science Foundation (Grants No.12274187, No.12047501, No.12274187, No.12247101, No. 11834005).

-
- [1] B. Keimer, S. A. Kivelson, M. R. Norman, S. Uchida, and J. Zaanen, From quantum matter to high-temperature superconductivity in copper oxides, *Nature* **518**, 179 (2015).
 - [2] C. Proust and L. Taillefer, The remarkable underlying ground states of cuprate superconductors, *Annual Review of Condensed Matter Physics* **10**, 409 (2019).
 - [3] J. Hubbard, Electron correlations in narrow energy bands, *Proc. R. Soc. A* **276**, 238 (1963).
 - [4] F. C. Zhang and T. M. Rice, Effective hamiltonian for the superconducting Cu oxides, *Phys. Rev. B* **37**, 3759 (1988).
 - [5] V. J. Emery, Theory of high- T_c superconductivity in oxides, *Phys. Rev. Lett.* **58**, 2794 (1987).
 - [6] J. E. Hirsch and S. Tang, Antiferromagnetism in the two-dimensional Hubbard model, *Phys. Rev. Lett.* **62**, 591 (1989).
 - [7] S. R. White, D. J. Scalapino, R. L. Sugar, E. Y. Loh, J. E. Gubernatis, and R. T. Scalettar, Numerical study of the two-dimensional Hubbard model, *Phys. Rev. B* **40**, 506 (1989).
 - [8] M. Qin, H. Shi, and S. Zhang, Benchmark study of the two-dimensional Hubbard model with auxiliary-field quantum monte carlo method, *Phys. Rev. B* **94**, 085103 (2016).
 - [9] A. Wietek, Y.-Y. He, S. R. White, A. Georges, and E. M. Stoudenmire, Stripes, antiferromagnetism, and the pseudogap in the doped Hubbard model at finite temperature, *Phys. Rev. X* **11**, 031007 (2021).
 - [10] E. Gull, O. Parcollet, and A. J. Millis, Superconductivity and the pseudogap in the two-dimensional Hubbard model, *Phys. Rev. Lett.* **110**, 216405 (2013).
 - [11] W. Wu, M. S. Scheurer, S. Chatterjee, S. Sachdev, A. Georges, and M. Ferrero, Pseudogap and fermi-surface topology in the two-dimensional Hubbard model, *Phys. Rev. X* **8**, 021048 (2018).
 - [12] C. Hille, D. Rohe, C. Honerkamp, and S. Andergassen, Pseudogap opening in the two-dimensional Hubbard model: A functional renormalization group analysis, *Phys. Rev. Research* **2**, 033068 (2020).
 - [13] G. Ehlers, S. R. White, and R. M. Noack, Hybrid-space density matrix renormalization group study of the doped two-dimensional Hubbard model, *Phys. Rev. B* **95**, 125125 (2017).
 - [14] M. Qin, C.-M. Chung, H. Shi, E. Vitali, C. Hubig, U. Schollwöck, S. R. White, and S. Zhang, Absence of superconductivity in the pure two-dimensional Hubbard model, *Phys. Rev. X* **10**, 031016 (2020).
 - [15] Y. F. Kung, E. A. Nowadnick, C. J. Jia, S. Johnston, B. Moritz, R. T. Scalettar, and T. P. Devereaux, Doping evolution of spin and charge excitations in the Hubbard model, *Phys. Rev. B* **92**, 195108 (2015).
 - [16] Z. Chen, Y. Wang, S. N. Rebec, T. Jia, M. Hashimoto, D. Lu, B. Moritz, R. G. Moore, T. P. Devereaux, and Z.-X. Shen, Anomalous strong near-neighbor attraction in doped 1d cuprate chains, *Science* **373**, 1235 (2021).
 - [17] K. Kuroki, T. Kimura, and H. Aoki, Quantum Monte Carlo study of the pairing correlation in the Hubbard ladder, *Phys. Rev. B* **54**, R15641 (1996).
 - [18] L. Balents and M. P. A. Fisher, Weak-coupling phase diagram of the two-chain Hubbard model, *Phys. Rev. B* **53**, 12133 (1996).
 - [19] R. Noack, S. White, and D. Scalapino, The ground state of the two-leg Hubbard ladder a density-matrix renormalization group study, *Physica C: Superconductivity* **270**, 281 (1996).
 - [20] S. Daul and D. J. Scalapino, Frustrated hubbard ladders and superconductivity in κ -BEDT-TTF organic compounds, *Phys. Rev. B* **62**, 8658 (2000).
 - [21] K. Louis, J. V. Alvarez, and C. Gros, Fermi surface renormalization in Hubbard ladders, *Phys. Rev. B* **64**, 113106 (2001).
 - [22] M. Tsuchiizu and A. Furusaki, Generalized two-leg Hubbard ladder at half filling: Phase diagram and quantum criticalities, *Phys. Rev. B* **66**, 245106 (2002).
 - [23] C. Degli Esposti Boschi, A. Montorsi, and M. Roncaglia, Brane parity orders in the insulating state of Hubbard ladders, *Phys. Rev. B* **94**, 085119 (2016).
 - [24] A. Nocera, Y. Wang, N. D. Patel, G. Alvarez, T. A. Maier, E. Dagotto, and S. Johnston, Doping evolution of charge and spin excitations in two-leg Hubbard ladders: Comparing DMRG and FLEX results, *Phys. Rev. B* **97**, 195156 (2018).
 - [25] L. F. Tocchio, F. Becca, and A. Montorsi, Superconductivity in the Hubbard model: a hidden-order diagnostics from the Luther-Emery phase on ladders, *SciPost Phys.* **6**, 018 (2019).

- [26] H.-C. Jiang, S. Chen, and Z.-Y. Weng, Critical role of the sign structure in the doped Mott insulator: Luther-Emery versus Fermi-liquid-like state in quasi-one-dimensional ladders, *Phys. Rev. B* **102**, 104512 (2020).
- [27] Y. Gannot, Y.-F. Jiang, and S. A. Kivelson, Hubbard ladders at small U revisited, *Phys. Rev. B* **102**, 115136 (2020).
- [28] B.-X. Zheng, C.-M. Chung, P. Corboz, G. Ehlers, M.-P. Qin, R. M. Noack, H. Shi, S. R. White, S. Zhang, and G. K.-L. Chan, Stripe order in the underdoped region of the two-dimensional Hubbard model, *Science* **358**, 1155 (2017).
- [29] S. D. Edkins, A. Kostin, K. Fujita, A. P. Mackenzie, H. Eisaki, S. Uchida, S. Sachdev, M. J. Lawler, E.-A. Kim, J. C. S. Davis, and M. H. Hamidian, Magnetic field induced pair density wave state in the cuprate vortex halo, *Science* **364**, 976 (2019).
- [30] P. Corboz, S. R. White, G. Vidal, and M. Troyer, Stripes in the two-dimensional t - J model with infinite projected entangled-pair states, *Phys. Rev. B* **84**, 041108 (2011).
- [31] A. S. Darmawan, Y. Nomura, Y. Yamaji, and M. Imada, Stripe and superconducting order competing in the Hubbard model on a square lattice studied by a combined variational monte carlo and tensor network method, *Phys. Rev. B* **98**, 205132 (2018).
- [32] K. Ido, T. Ohgoe, and M. Imada, Competition among various charge-inhomogeneous states and d -wave superconducting state in hubbard models on square lattices, *Phys. Rev. B* **97**, 045138 (2018).
- [33] T. I. Vanhala and P. Törmä, Dynamical mean-field theory study of stripe order and d -wave superconductivity in the two-dimensional hubbard model, *Phys. Rev. B* **97**, 075112 (2018).
- [34] B. Ponsioen, S. S. Chung, and P. Corboz, Period 4 stripe in the extended two-dimensional Hubbard model, *Phys. Rev. B* **100**, 195141 (2019).
- [35] J. M. Tranquada, B. J. Sternlieb, J. D. Axe, Y. Nakamura, and S. Uchida, Evidence for stripe correlations of spins and holes in copper oxide superconductors, *Nature* **375**, 561 (1995).
- [36] J. M. Tranquada, H. Woo, T. G. Perring, H. Goka, G. D. Gu, G. Xu, M. Fujita, and K. Yamada, Quantum magnetic excitations from stripes in copper oxide superconductors, *Nature* **429**, 534 (2004).
- [37] Y. Kohsaka, C. Taylor, K. Fujita, A. Schmidt, C. Lupien, T. Hanaguri, M. Azuma, M. Takano, H. Eisaki, H. Takagi, S. Uchida, and J. C. Davis, An intrinsic bond-centered electronic glass with unidirectional domains in underdoped cuprates, *Science* **315**, 1380 (2007).
- [38] H.-C. Jiang and T. P. Devereaux, Superconductivity in the doped Hubbard model and its interplay with next-nearest hopping t' , *Science* **365**, 1424 (2019).
- [39] C.-M. Chung, M. Qin, S. Zhang, U. Schollwöck, and S. R. White (The Simons Collaboration on the Many-Electron Problem), Plaquette versus ordinary d -wave pairing in the t' -Hubbard model on a width-4 cylinder, *Phys. Rev. B* **102**, 041106 (2020).
- [40] Y.-F. Jiang, J. Zaanen, T. P. Devereaux, and H.-C. Jiang, Ground state phase diagram of the doped Hubbard model on the four-leg cylinder, *Phys. Rev. Research* **2**, 033073 (2020).
- [41] X. Hao, C. Chia-Min, Q. Mingpu, U. Schollwöck, R. W. Steven, and S. Zhang, Coexistence of superconductivity with partially filled stripes in the Hubbard model, [arXiv:2303.08376](https://arxiv.org/abs/2303.08376) (2023).
- [42] M. Hirayama, Y. Yamaji, T. Misawa, and M. Imada, Ab initio effective Hamiltonians for cuprate superconductors, *Phys. Rev. B* **98**, 134501 (2018).
- [43] M. Hirayama, T. Misawa, T. Ohgoe, Y. Yamaji, and M. Imada, Effective Hamiltonian for cuprate superconductors derived from multiscale ab initio scheme with level renormalization, *Phys. Rev. B* **99**, 245155 (2019).
- [44] M. Uehara, T. Nagata, J. Akimitsu, H. Takahashi, N. Môri, and K. Kinoshita, Superconductivity in the ladder material $\text{Sr}_{0.4}\text{Ca}_{13.6}\text{Cu}_{24}\text{O}_{41.84}$, *J. Phys. Soc. Jpn* **65**, 2764 (1996).
- [45] J. H. Schön, M. Dorget, F. C. Beuran, X. Z. Xu, E. Arushanov, M. Laguës, and C. D. Cavellin, Field-induced superconductivity in a spin-ladder cuprate, *Science* **293**, 2430 (2001).
- [46] N. Fujiwara, N. Môri, Y. Uwatoko, T. Matsumoto, N. Motoyama, and S. Uchida, Pressure-induced superconductivity in the spin-ladder cuprate, *Journal of Physics: Condensed Matter* **17**, S929 (2005).
- [47] Y. Wang, Z. Chen, T. Shi, B. Moritz, Z.-X. Shen, and T. P. Devereaux, Phonon-mediated long-range attractive interaction in one-dimensional cuprates, *Phys. Rev. Lett.* **127**, 197003 (2021).
- [48] A. Amaricci, A. Camjayi, K. Haule, G. Kotliar, D. Tanasković, and V. Dobrosavljević, Extended hubbard model: Charge ordering and Wigner-Mott transition, *Phys. Rev. B* **82**, 155102 (2010).
- [49] L. Huang, T. Ayral, S. Biermann, and P. Werner, Extended dynamical mean-field study of the Hubbard model with long-range interactions, *Phys. Rev. B* **90**, 195114 (2014).
- [50] H. Terletska, T. Chen, and E. Gull, Charge ordering and correlation effects in the extended Hubbard model, *Phys. Rev. B* **95**, 115149 (2017).
- [51] M. Vandelli, V. Harkov, E. A. Stepanov, J. Gukelberger, E. Kozik, A. Rubio, and A. I. Lichtenstein, Dual boson diagrammatic Monte Carlo approach applied to the extended Hubbard model, *Phys. Rev. B* **102**, 195109 (2020).
- [52] H. Terletska, S. Isakov, T. Maier, and E. Gull, Dynamical cluster approximation study of electron localization in the extended Hubbard model, *Phys. Rev. B* **104**, 085129 (2021).
- [53] S. R. White, Density matrix formulation for quantum renormalization groups, *Phys. Rev. Lett.* **69**, 2863 (1992).
- [54] S. R. White, Density-matrix algorithms for quantum renormalization groups, *Phys. Rev. B* **48**, 10345 (1993).
- [55] U. Schollwöck, The density-matrix renormalization group, *Rev. Mod. Phys.* **77**, 259 (2005).
- [56] U. Schollwöck, The density-matrix renormalization group in the age of matrix product states, *Annals of Physics* **326**, 96 (2011), january 2011 Special Issue.
- [57] A. Luther and V. J. Emery, Backward scattering in the one-dimensional electron gas, *Phys. Rev. Lett.* **33**, 589 (1974).
- [58] M. Fishman, S. R. White, and E. M. Stoudenmire, The itensor software library for tensor network calculations, *SciPost Phys. Codebases*, 4 (2022).
- [59] M. Jiang, Enhancing d -wave superconductivity with nearest-neighbor attraction in the extended Hubbard model, *Phys. Rev. B* **105**, 024510 (2022).
- [60] D.-W. Qu, B.-B. Chen, H.-C. Jiang, Y. Wang, and W. Li, Spin-triplet pairing induced by near-neighbor attraction in the extended Hubbard model for cuprate chain, *Commun. Phys.* **5**, 257 (2022).
- [61] C. Peng, Y. Wang, J. Wen, Y. Lee, T. Devereaux, and H.-C. Jiang, Enhanced superconductivity by near-neighbor attraction in the doped Hubbard model, [arXiv:2206.03486](https://arxiv.org/abs/2206.03486) (2022).
- [62] T. Tang, B. Moritz, C. Peng, Z. X. Shen, and T. P. Devereaux, Traces of electron-phonon coupling in one-dimensional cuprates, [arXiv:2210.09288](https://arxiv.org/abs/2210.09288) (2022).
- [63] H.-X. Wang, Y.-M. Wu, Y.-F. Jiang, and H. Yao, Spectral properties of 1d extended Hubbard model from bosonization and time-dependent variational principle: applications to 1D cuprate, [arXiv:2211.02031](https://arxiv.org/abs/2211.02031) (2022).